Macromolecules

Article

pubs.acs.org/Macromolecules

High-Contrast Visualization and Differentiation of Microphase Separation in Polymer Blends by Fluorescent AIE Probes

Ting Han,[†,‡] Chen Gui,[†,‡] Jacky W. Y. Lam,[†,‡] Meijuan Jiang,[†,‡] Ni Xie,[†,‡] Ryan T. K. Kwok,[†,‡] and Ben Zhong Tang*[,†,‡,§]

[†]Guangdong Provincial Key Laboratory of Brain Science, Disease and Drug Development, HKUST-Shenzhen Research Institute, No. 9 Yuexing first RD, South Area, Hi-tech Park, Nanshan, Shenzhen 518057, China

[‡]Department of Chemistry, Hong Kong Branch of Chinese National Engineering Research Center for Tissue Restoration and Reconstruction, Institute for Advanced Study, Institute of Molecular Functional Materials, Division of Biomedical Engineering, Division of Life Science and State Key Laboratory of Molecular Neuroscience, The Hong Kong University of Science & Technology, Clear Water Bay, Kowloon, Hong Kong

[§]Guangdong Innovative Research Team, SCUT-HKUST Joint Research Laboratory, State Key Laboratory of Luminescent Materials and Devices, South China University of Technology, Guangzhou 510640, China

Supporting Information

ABSTRACT: The visualization of microphase separation in immiscible polymer blends is of great academic and industrial significance as the phase-separated structures are directly associated with the properties and performances of the blend materials and ultimately influence the corresponding product quality. However, conventional techniques for detecting microphase separation are generally expensive and time-consuming with troublesome and even destructive sample preparation procedures. Complicated and highly material-dependent chemical reactions or interactions are often involved in some characterization approaches. In this work, we demonstrated a simple, fast, and powerful method for high-contrast visualization and differentiation of micrometer-sized phase separation in polymer blends using luminogens with aggregation-induced emission characteristics (AIEgens) as fluorescent probes. This method relies on the sensitive fluorescence response of AIEgens to the change of environmental rigidity and polarity and operates based on the mechanisms of "restriction of intramolecular motions" and "twisted intramolecular charge transfer". The working principle indicates that this visualization strategy is applicable to a wide scope of polymer blends comprised of components with different rigidities and/or polarities.

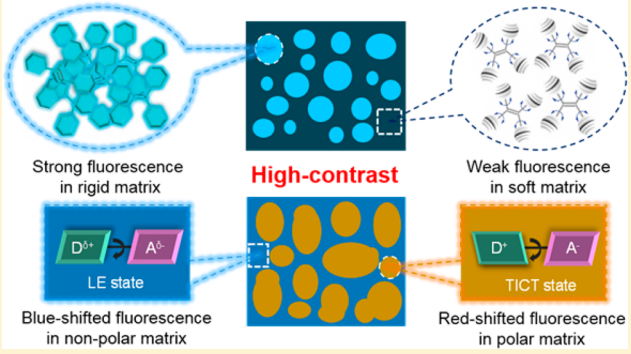

INTRODUCTION

Polymeric materials play an essential and ubiquitous role in our daily life. They are widely used in packaging, housewares, paint, pipes, fabric, automotive parts, biomedical supplies, etc. To meet the application requirements in various fields, blending has been commonly used in polymer technology to generate new materials by simply mixing two or more polymers together. The resulting blends generally possess more desirable structural and physical characteristics in the solid state than those of individual components.[1,2] Nevertheless, the vast majority of polymer blends are immiscible and will easily and inevitably undergo phase separation process.[3,4] The phase-separated structures greatly affect the macroscopic properties, such as toughness, processability, transparency, chemical and weather resistance, thermal stability, flowability, etc., of a material and have strong impact on the performance of the corresponding products.[5,6] Especially for polymer blend films used in optoelectronic devices, the morphology and domain size of the microphase separation have a direct effect on their electrical and mechanical properties and hence the device performances.[7−10] Therefore, it is of considerable academic and industrial significance to detect the phase-separated structure in a polymer blend, so as to understand the underlying morphology−performance relationship and ultimately to realize a control on the performance of immiscible polymer mixtures by manipulating their phase separation.

To achieve this goal, various modern microscopic and spectroscopic approaches have been applied,[11−15] and among them, scanning electron microscopy (SEM), transmission electron microscopy (TEM), and atomic force microscopy are the most commonly used characterization techniques.[16] However, these methods are generally expensive and time-

Received: May 11, 2017
Revised: July 8, 2017
Published: July 24, 2017

DOI: 10.1021/acs.macromol.7b00973
Macromolecules 2017, 50, 5807−5815

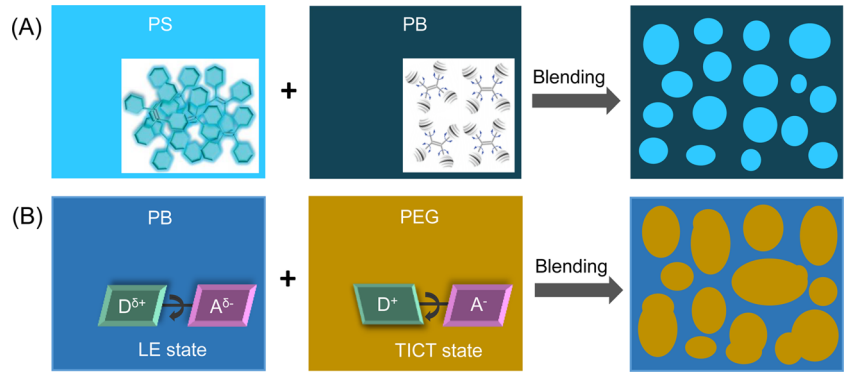

Figure 1. Schematic representation of the proposed working mechanisms for the visualization of phase-separated morphology in polymer blends using fluorescent AIE probes. (A) AIEgens based on RIM mechanism are possible to visualize and differentiate polymer blends with different rigidities by the variation in emission intensity. (B) AIEgens with TICT properties may be capable of distinguishing polymer blends with different polarities by the different emission colors in respective polymer component.

consuming for industrial applications, and skillful technicians are often required to operate the instruments.[17] In addition, the sample preparation procedures are often troublesome and may irreversibly change or even damage the sample. For example, the specimen for TEM analysis needs to be pretreated by time-consuming and challenging cryo-ultramicrotomy to make it thin enough to be electron transparent. On the other hand, to enhance the contrast of heterophase polymers, selective chemical staining using heavy-metal compounds, such as osmium tetroxide and ruthenium tetroxide, is generally required, which is very toxic and can introduce artifacts to the specimen.[16,18,19] In most cases, the identification of polymer components in a blend are realized indirectly either by their mechanical property difference or by selective phase removal by certain solvents.[20,21] Concerning the intrinsic limitations of the existing strategies, the development of a simple and powerful tool for the direct visualization and differentiation of microphase separation is thus critically important and highly desirable.

Fluorescence-based techniques have the advantages of high sensitivity, large contrast, visible detection, and fast response. Although fluorescence microscopy has been widely used in life science for biological sensing and imaging, it is much less explored in polymer research. The lack of efficient fluorescent labels for polymeric materials may be a possible reason. As most of the commodity polymers are inherently nonfluorescent or show very weak fluorescence, thus similar to bioimaging, external fluorophores are needed to label the polymers to allow their observation under fluorescence microscope. In this regard, one known strategy is the covalent introduction of fluorescent moiety to polymer, which, however, involves fussy polymerization design and complicated synthetic procedure.[22−24] A simple alternative way is to disperse low-molecular-weight dye molecules in the polymer blend. Nevertheless, conventional fluorophores often suffer from fluorescence quenching with increasing concentration due to the notorious aggregation-caused quenching (ACQ) effect.[25,26] Meanwhile, the characterization of phased-separated structures using conventional ACQ fluorophores generally relies on the selective introduction of dye molecules to one polymer component by chemical interactions, which is not workable for blend systems where both polymer matrices exhibit similar interactions with the fluorophore moiety.[23,27] On the other hand, luminogens with aggregation-induced emission characteristics (AIEgens) show intense emission when their intramolecular motions are restricted, and their emissions are very sensitive to the change of their surrounding microenvironments. Since the first report in 2001 by our group, AIEgens have attracted tremendous attention and have found many applications.[28,29] Until now, a large variety of AIEgens have been developed, and some are even commercialized. AIEgen-based imaging systems possess the merits of large absorptivity, high brightness in the solid state, low background noise, etc. In addition to bioimaging, AIEgens have been used for the direct and high-contrast visualization of breath-figure formation,[30] gelation process,[31] microscopic damage,[32] macrodispersion of inorganic fillers in organic−inorganic composites,[33] etc. Previously, we have reported a chemical-staining method to detect the micrometer-sized morphology of polymer blends comprising a noncoordinating polymer and a Lewis-basic polymer by using a Lewis-acidic AIEgen.[17] However, such method is based on the chemical reactions between the functional group in the AIEgen and the reaction site on the polymer component, which is material-dependent and is only suitable for a limited scope of polymer blends.

In this work, we demonstrated a proof-of-concept study on a simple, low-cost, time-saving, and more general fluorescent method for high-contrast observation and direct differentiation of phase-separated morphology in polymer blends based on the sensitive photophysical change of AIEgens in different polymer phases. By utilizing the presented method, phase structures of various immiscible polymer blends, such as polystyrene (PS)/polybutadiene (PB), poly(methyl methacrylate) (PMMA)/PB, and poly(ethylene glycol) (PEG)/PB, can be easily and clearly observed. The effects of blend ratios, polymer concentrations, and molecular weights on the phase morphologies of PS/PB thin films were systematically investigated and the formation of phase-separated structure in PS/PB blend film during the solvent evaporation of its preparation process was dynamically visualized and monitored, which are hard to be achieved by conventional characterization techniques. The details of the design concept and the corresponding experimental verification and applications of this method will be discussed in turns.

RESULTS AND DISCUSSION

On the basis of the working mechanism of AIE, we proposed a possible design concept, as schematically illustrated in Figure 1, for fluorescence visualization of microphase separation in polymer blends by using AIEgens. Polymer blends composed of rigid (plastic) and soft (rubber) components are commonly

DOI: 10.1021/acs.macromol.7b00973
Macromolecules 2017, 50, 5807−5815

used in polymer industry to tune the mechanical properties of products. Such polymer blends are commercialized as themoplastic elastomers or as rubber-toughened plastics.[34] For example, PS is a very stiff and brittle material, whereas PB is rubbery and can absorb energy under stress. By blending PS with a small amount of PB, the resulting polymer is known as high-impact polystyrene and is tougher, more ductile, and less likely to break upon bending than the unmodified one. However, the phase-separated structure of PS/PB blend is hard to be detected by electron microscopy without toxic chemical staining. Additionally, there is no reactive functional group present in PS or PB. Thus, fluorescent imaging based on chemical-sensing mechanism is not applicable. The restriction of intramolecular motions (RIM) is a well-accepted working mechanism for the AIE phenomenon,[35] which allows AIEgens to exhibit different emission behaviors in response to the local rigidities of their surrounding microenvironments. As shown in Figure 1A, when AIEgens with multiple molecular rotors are dispersed in a glassy or rigid polymer matrix, the restriction of their intramolecular motions makes them show strong emission upon photoexcitation. Conversely, when AIEgens are mixed in a rubbery or soft polymer matrix, the movement of the polymer segments at room temperature and relatively large free volume between the polymer chains will enable the AIEgens to undergo intramolecular motions with little constraint. These dynamic motions will nonradiatively dissipate the exciton energy and quench their light emission.[36,37] Considering the distinct difference in the emission intensity of AIEgens in different polymer environments, we envisioned that AIEgens based on RIM mechanism are promising fluorescent probes for the visualization and differentiation of the microphase separation of polymer blends with different rigidities, such as the PS/PB mixture. Meanwhile, polymer blends comprising components with different polarities are also widely investigated. These materials have found many applications in tissue engineering, drug delivery, biomedical materials, etc.,[19,38−41] as their biocompatibility and biodegradability can be controlled by tuning the hydrophobic/hydrophilic compositions in the blend or by selecting polymer components with proper polarity difference.[42−44] This type of polymer blend may be composed of homopolymers with similar rigidities, such as PB and PEG. As such, the RIM mechanism may not function well as an indicator in this system. Thanks to the big and diversified AIE toolbox,[28] AIEgens with twisted intramolecular charge transfer (TICT) effect may be capable of solving such a challenge. The emission color of AIEgens with electron donor (D) and acceptor (A) units often changes with the environmental polarity due to the TICT effect.[45,46] Inspired by the solvatochromism of TICT-active AIEgens, we envisioned that in a nonpolar polymer matrix the AIEgen will be in the locally excited (LE) state with its D and A units existing in an almost parallel fashion. In a polar polymer environment, however, the excited state of a D−A-type luminogen will undergo a geometry rearrangement by intramolecular rotation. This brings the D and A units into a twisted conformation and leads to a total charge separation. The luminogen is now located at the TICT state, and as the bandgap of the TICT state is narrower than that of the LE state, the emission of the dye molecule will red-shift in a polar polymer matrix (Figure 1B). Based on this assumption, the TICT-active AIEgens are anticipated to be able to distinguish polymer blends with different polarities by the different emission colors in respective polymer component.

To demonstrate our design concept, commercially available AIEgens, namely tetraphenylethene (TPE) and triphenylamine-substituted [(*Z*)-4-benzylidene-2-methyloxazol-5(4*H*)-one] (TPABMO), were selected as the representative staining reagents based on RIM and RIM + TICT mechanisms, respectively, to dope with the commodity polymer blends of PS, PB, PMMA, and PEG. Their structures are provided in Schemes S1 and S2.

The general experimental workflow is illustrated in Figure 2, and the experimental details can be found in the Supporting Information. First, a polymer blend solution was prepared by well mixing the solution of each polymer component, into which the as-prepared AIEgen solution was subsequently added to mix with the polymer blend, generating a homogeneous polymer/AIEgen mixture under ultasonication. Afterward, uniform thin films were fabricated by spin-coating the blend solution onto quartz plates. During spin-coating, the fast evaporation of solvent will lead to the easy formation of separated binary phase in the polymer blend film. Last, the morphology of the blend films was observed under a fluorescent microscope. The whole experimental procedure is quite simple and time-saving and involves no sample destruction step.

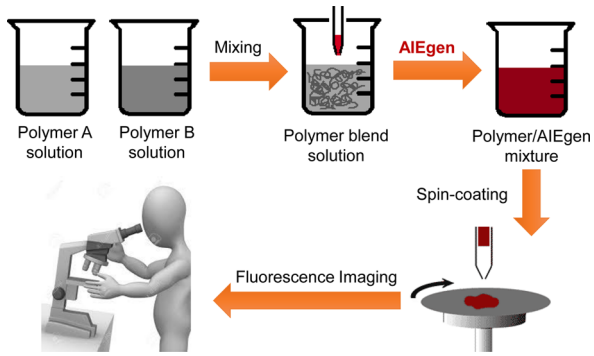

Figure 2. Experimental workflow: (1) physically mixing AIEgens with polymers, (2) preparing polymer blend thin films by solution spin-coating, and (3) subsequent observation under a fluorescent microscopy.

The TPE/PS/PB system serves first as a model system to test the feasibility of our design principle in Figure 1A and meanwhile provides feedback for further optimization of the experimental condition. In an initial attempt, 1.0 wt % TPE was doped in the thin films of pure PS, pure PB, and PS/PB blend with a mass fraction of PB (w_{PB}) of 50%, respectively. As shown in Figure S1, the TPE/PS film emits much stronger photoluminescence (PL) with a higher fluorescence quantum yield (Φ_F = 19.6%) than that of TPE/PB (Φ_F = 1.7%). Encouraged by this result, we then investigated the phase morphology of these TPE/polymer films using a fluorescent microscope. While the bright-field and fluorescent images of TPE/PS and TPE/PB films show smooth surface topography (Figures 3A−3A2 and 3B−3B2), a clear and high-contrast spatial distribution of phase-separated morphology was observed in the images of TPE/PS/PB blend with a large field of view (Figure 3C−3C2). Notably, when viewed under UV irradiation, an even distribution of brightly emissive spherical domains was seen in a faintly emissive matrix. Because the TPE/PS film exhibits a much stronger emission than that of TPE/PB, it is unambiguous to assign the brightly

DOI: 10.1021/acs.macromol.7b00973
Macromolecules 2017, 50, 5807−5815

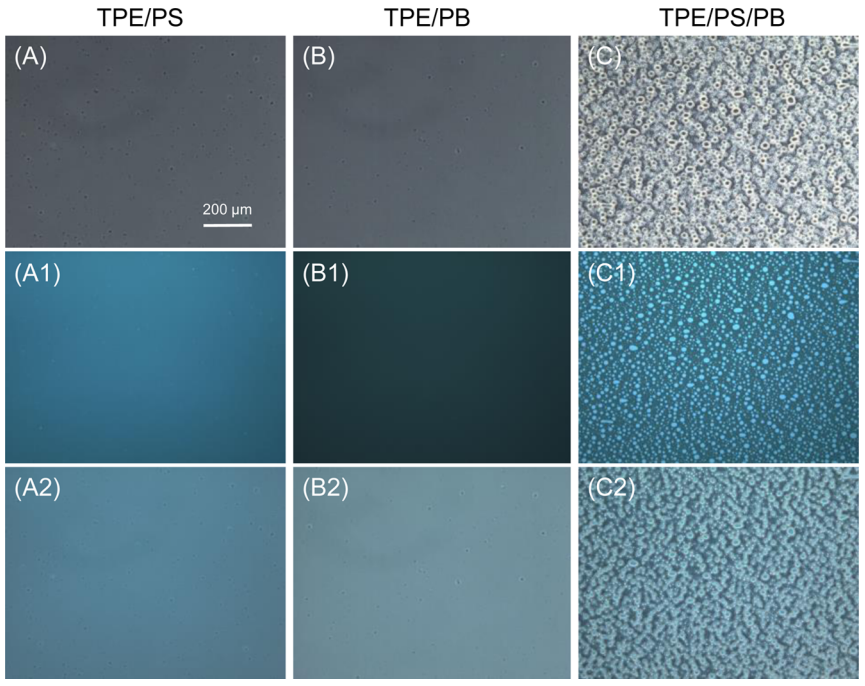

Figure 3. (A–C) Bright-field, (A1–C1) fluorescent, and (A2–C2) merged images of 1.0 wt % TPE-doped PS, PB, and PS/PB (50/50, w/w) films. Scale bar: 200 μm.

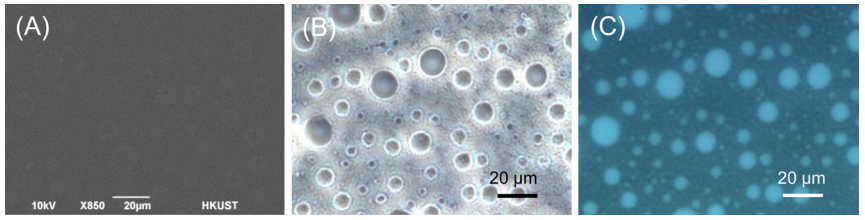

Figure 4. (A) SEM image, (B) bright-field image, and (C) fluorescent image of 1.0 wt % TPE-doped thin film of PS/PB (50/50, w/w).

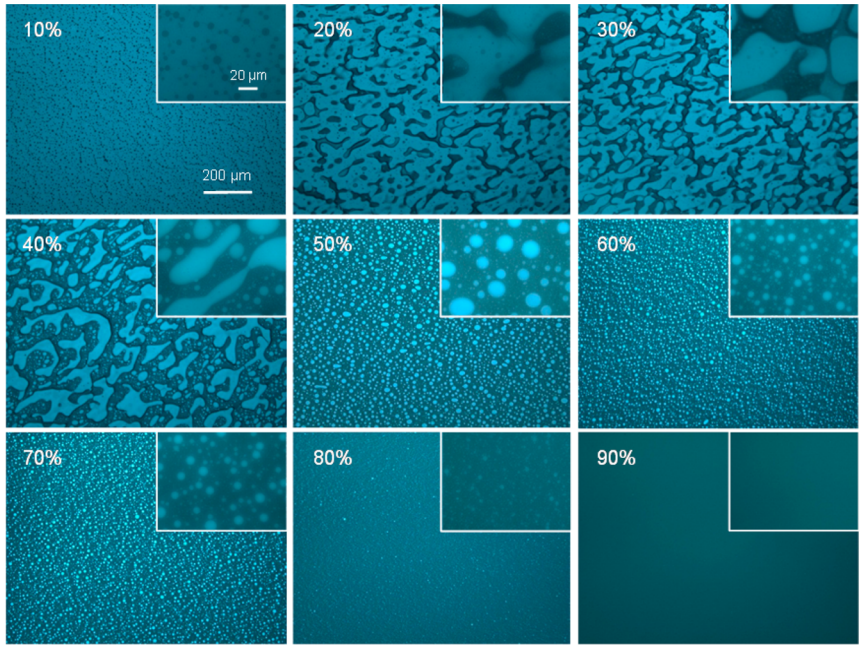

Figure 5. Fluorescent images of 1.0 wt % TPE-doped thin films of PS/PB blends with different mass fractions of PB (w_{PB}). Scale bar: 200 μm (main) and 20 μm (inset).

DOI: 10.1021/acs.macromol.7b00973
Macromolecules 2017, 50, 5807–5815

emissive "isolated islands" with diameters of 4−28 μm as PS-rich domains, which are surrounded by the continuous and weakly emissive PB phase. The merged image in Figure 3C2 clearly reveals the correspondence between the bright-field morphology and the fluorescent pattern of the dye-doped blend film. To test the dye's capability, we decreased the doping concentration to 0.1 wt %. As indicated by the results given in Figure S2, clear microphase separation was still observed in the PS/PB blend, but the contrast is not as good as that at high doping concentration. Thus, 1.0 wt % was chosen as a suitable probe concentration for the following investigation.

To demonstrate the advantage of the present method over the traditional ones, SEM measurement on the same TPE/PS/PB film was conducted. As the polymer specimen is nonconductive, an ultrathin gold layer was first coated on its surface by high-vacuum evaporation. However, after the expensive and troublesome sample treatment, only a SEM image with an ambiguous phase-separated morphology in poor contrast was obtained (Figure 4A). Although the bright-field image taken by the phase-contrast microscopy shows a clear phase-separated structure (Figure 4B), it cannot provide detailed information on the blend composition. Additionally, the bright-field morphology may give misleading information due to the inherent roughness of the film and the interference by the optical effect. For instance, the circle domains in Figure 4B can be either hollow microtubes or solid spheres. Now, these shortcomings can be overcome by fluorescence imaging using AIEgens. The fluorescent image shown in Figure 4C provides more valuable and detailed insights into the microscopic morphology of PS/PB without the problems stated above. The three-dimensional fluorescent images of the thin film of PS/PB further confirmed its phase-separated structure where the PS-rich spherical domains were embedded in the continuous PB-rich phase (Figure S3 and Videos S1 and S2). On the other hand, the present method also enables direct and easy differentiation of the domain composition by the obvious difference in the emission intensity of the AIEgen in different phases.

On the basis of the preliminary results, we then further utilized this fluorescence imaging method to systematically investigate the microphase separation in PS/PB mixtures with different blend ratios. As indicated by Figure 5, the phase-separated morphology and domain size of PS/PB are strongly affected by the blend ratio. In a thin film of PS/PB blend with w_{PB} of 10%, uniform dispersion of faintly emissive PB domains in a brightly emissive PS matrix was observed. PS is the major component in this case, and PB separates from the PS phase as small and round-shaped domains. As w_{PB} increases, the isolated PB spheres tend to coalesce together to form large domains and finally generate irregular domain structures. Bicontinuous interpenetrating networks appear when w_{PB} reaches 30%. Further increment of w_{PB} to 40% leads to a reversed morphology: the blue emissive PS phase is embedded in a dark PB matrix, and PS becomes a minor component. Both irregular-shaped and spherical PS domains are observed in one image. At w_{PB} of 50%, all the PS domains are spherical in shape. With the gradual increase of PB fraction from 60% to 80%, the average size of the island-like PS domains becomes smaller and smaller. At 90% w_{PB}, the PS domains are hard to be observed because their size is probably smaller than the spatial resolution limit (about 200 nm) of traditional microscopy. In addition, the effects of polymer concentration and molecular weight on the phase morphologies of PS/PB thin films were also studied by this approach. The fluorescent image in Figure S4A suggested that when the polymer concentration of the coating solution was lowered from 42 to 17 mg/mL, the phase shape of the PS/PB thin film with w_{PB} of 50% remained almost unchanged with uniform spherical PS domains dispersing in the continuous PB phase. However, the average diameter of the PS domains significantly decreased from ∼17 to ∼7 μm. Phase separation can also be clearly observed in PS/PB blend (50/50, w/w) comprised of PS with low molecular weight (M_w = 42 000 g/mol) (Figure S4B), in which the PS domains appear as granular morphology with an average diameter of ∼8 μm. These results are consistent with the general rule that smaller domains will be generated in the phase structures of spin-coated thin films at lower polymer concentration and lower molecular weight.[7]

The above-mentioned results demonstrate that it is a good strategy to use AIEgens with rotors for clear analysis of the spatial distribution and phase composition of polymer blends with different rigidities by the difference in emission intensity. We then verified the feasibility of the design principle in Figure 1B, in which the emission color serves as an indicator for the phase composition in a polymer blend. TPABMO is an AIEgen with both molecular rotors and D−π−A structure (Scheme S1).[47] This luminogen is found to be very sensitive to the change of environmental polarity. Its emission color undergoes a significant red-shift with increasing the solvent polarity due to the strong TICT effect (Figure 6A). Even there is a small change in polarity when changing the solvent from hexane to toluene, distinct color variation from blue to green was still observed. Inspired by this, we doped 1.0 wt % TPABMO to stain polymers with different structural polarities, including PB, PS, PMMA, and PEG. The PL behaviors of these TPABMO-doped homopolymer films were first investigated. Delightfully, TPABMO also shows a sensitive response to the polarity change in the polymer matrix. As depicted in Figure 6B, TPABMO emits blue and orange color at 499 and 567 nm in nonpolar PB and relatively polar PEG matrix, respectively, while TPABMO/PS and TPABMO/PMMA films are green emissive at 512 and 525 nm, respectively. It is surprising to find out that a subtle difference in the structural polarity between PS and PB can result in such an obvious change in the emission color of TPABMO.

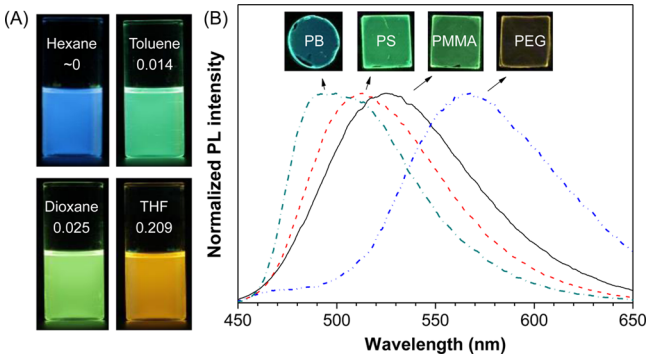

Figure 6. (A) Photographs of TPABMO in solvents with different polarities taken under UV irradiation. Δf = solvent polarity parameter. Δf = ∼0 (hexane), 0.014 (toluene), 0.025 (dioxane), and 0.209 (THF). Solution concentration: 10 μM. (B) Emission spectra of 1.0 wt % TPABMO-doped polymer films. Excitation wavelength: 410 nm. Inset: photos of TPABMO-doped polymer films taken under 365 nm UV irradiation from a hand-held UV lamp.

DOI: 10.1021/acs.macromol.7b00973
Macromolecules 2017, 50, 5807−5815

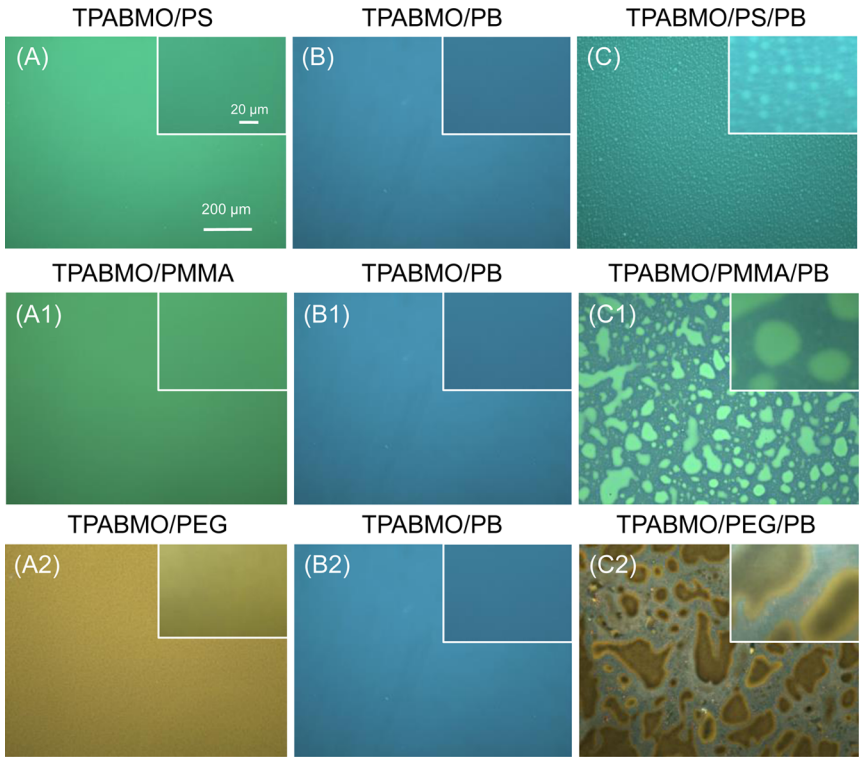

Figure 7. Fluorescent images of 1.0 wt % TPABMO-doped thin films of (A–C) PS, PB, and PS/PB (50/50, w/w), (A1–C1) PMMA, PB, and PMMA/PB (50/50, w/w), and (A2–C2) PEG, PB, and PEG/PB (50/50, w/w). Scale bar: 200 μm (main) and 20 μm (inset).

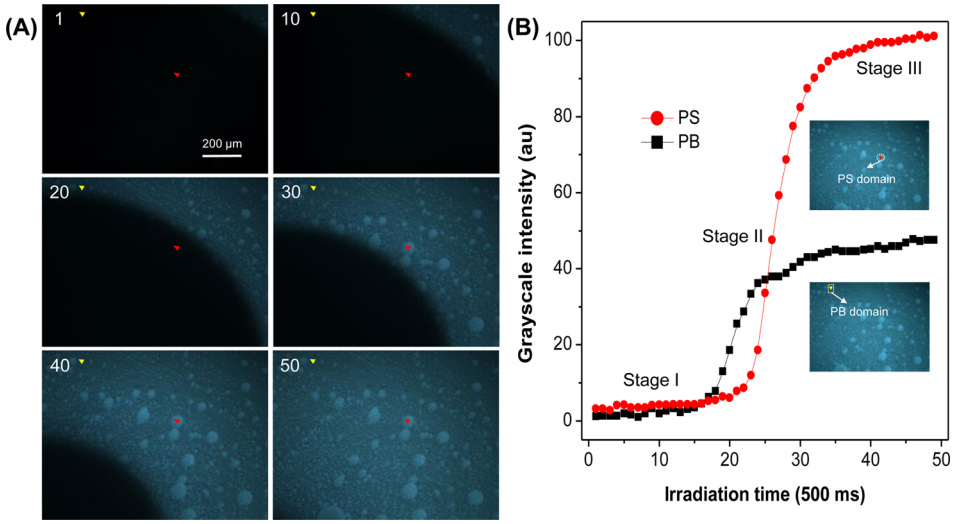

Figure 8. (A) Following the phase structure formation of PS/PB blend by adding one drop of its solution (50/50, w/w) with 1.0 wt % TPE on a quartz plate followed by photo taking at different scans. The scan number of each image is shown on the upper left corner, and additional information is provided in Video S3. Irradiation time: 500 ms/scan. (B) Plots showing the change of grayscale intensity in the chosen areas (as labeled by red and yellow arrows in (A)) with the increase of the irradiation time. Inset: fluorescence images indicating the phase composition.

The morphologies of PS/PB, PMMA/PB, and PEG/PB blends stained by TPABMO were then investigated using a fluorescence microscope (Figure 7). The images of TPABMO-doped homopolymers all show smooth morphology. In contrast, clear phase-separated structures were observed in the images of polymer blends. Different from the TPE probe which operates in the RIM mechanism, the phase composition in this case is identified by comparing the emission color of TPABMO in each domain with that of the corresponding homopolymers. For example, from the fluorescent image of TPABMO/PS/PB, we can easily point out that the green-emissive spherical domains are responsible for the PS phase and the blue-emissive continuous matrix belongs to the PB phase (Figure 7A–C and Figure S5). A similar phenomenon was observed in the TPABMO/PMMA/PB system, where the green-emissive irregular PMMA domains are surrounded by continuous, blue emissive PB matrix (Figure 7A1–C1 and Figure S6).

For polymer blends comprising components with both different polarities and different rigidities, both TPE and

DOI: 10.1021/acs.macromol.7b00973
Macromolecules 2017, 50, 5807–5815

TPABMO work well to visualize their phase-separated structures. However, for polymer blends composed of homopolymers with similar rigidities but different polarities, such as PEG/PB blend, TPABMO will be a more suitable candidate. As indicated in Figure 7A2−C2 and Figure S7, the TPABMO-stained PEG/PB blend shows a high-contrast and well-resolved phase separation structure with dual colors. By comparison with the emission color of TPABMO in pure PEG and PB, the orange emissive, irregular-shaped, and large-sized domains should be the PEG-rich phase, which is embedded in the blue emissive continuous PB phase.

To further extend the applications of this AIE technique, we then tested the possibility of using the presented method to visualize and monitor the formation of phase-separated morphology from the PS/PB blend solution during solvent evaporation in a dynamic fashion. One drop of AIEgen/PS/PB blend solution was added on a quartz plate followed by immediate observation under a fluorescence microscope. The grayscale intensity values of a certain domain in the corresponding images were calculated using a NIS-Elements microscope imaging software. When TPE was used as the fluorescent probe (Figure 8 and Video S3), the blend solution keeps almost nonemissive at the beginning, and no phase separation is detected (stage I). Once the solvent starts to evaporate, the viscosity of the solution rises and the phase-separated morphology can be clearly visualized. The corresponding emission intensity in the chosen area will also increase accordingly (stage II). With gradual solvent evaporation, the formed phase morphology basically remains the same. After the solvent is completely evaporated, the emission intensity in each domain will keep essentially unchanged (stage III). In the phase-separated structure, TPE always shows stronger emission in PS-rich domains than that in PB-rich continuous phase due to the RIM mechanism. TPABMO is also demonstrated to be suitable for such an application but using emission color as an indicator for the phase evolution (Figure S8 and Video S4). These results suggest that the presented AIE method is able to directly visualize and monitor the structure formation via polymer demixing in drop-casting films, which is hard to be achieved by other commonly used characterization techniques.

CONCLUSION

In summary, this work provides an expedient, time-saving, and powerful visualization method of micrometer-sized phase separation in polymer blends by using AIEgens as fluorescent probes. The domain structure and composition of a polymer mixture can be readily identified with high-contrast and low background noise by comparing the fluorescence properties, including the emission brightness and emission color, of AIEgens in each domain with those of the associated homopolymers. This detection method is simply based on the physical property change of AIEgens in different polymer matrices. No destructive, complicated, and material-dependent chemical reaction or modification is involved. The sample preparation procedure is facile and noninvasive. With these superior advantages over traditional analytical methods, the present visualization strategy is helpful to expedite the process for studying phase separation morphologies, dynamics, and mechanisms in various polymer blends in both academic and industrial areas. This work will not only widen the application of conventional fluorescence microscopy in polymer research but also facilitate the use of AIEgens as fluorescent probes in more advanced observation instruments, such as near-field scanning optical microscopy[36] and super-resolution techniques, thereby achieving nanostructured imaging of a wide variety of polymer blends by monitoring the fluorescence of AIEgens. Further extension of the scope of AIEgens to be applied in this method is undergoing in our lab.

ASSOCIATED CONTENT

Supporting Information

The Supporting Information is available free of charge on the ACS Publications website at DOI: 10.1021/acs.macromol.7b00973.

Structures of AIEgens and polymers; emission spectra and fluorescence quantum yields of 1.0 wt % TPE in PS and PB films; bright-field images, fluorescent images, and the corresponding merged images of 0.1 wt % TPE-doped thin films of PS, PB, and PS/PB (50/50, w/w); bright-field images and the corresponding merged images of 1.0 wt % TPABMO-doped thin films of PS, PMMA, PEG, PB, PS/PB (50/50, w/w), PMMA/PB (50/50, w/w), and PEG/PB (50/50, w/w); fluorescent 3D images constructed from the 2D confocal images of phase-separated structure of thin film of TPE-doped PS/PB (50/50, w/w) obtained on a laser scanning confocal microscope; fluorescent images of 1.0 wt % TPE-doped thin films of PS/PB blends (50/50, w/w) fabricated from a polymer concentration of 17 mg/mL and PS with a molecular weight of 42 000, respectively; representative fluorescent images of the PS/PB blend (50/50, w/w) containing 1.0 wt % TPABMO taken during the solvent evaporation of its preparation process and at different scans (PDF)

Videos S1−S4 (ZIP)

AUTHOR INFORMATION

Corresponding Author

*(B.Z.T.) E-mail tangbenz@ust.hk; Ph +852-2358-7375; Fax +852-2358-1594.

ORCID

Ting Han: 0000-0003-1521-6333

Ben Zhong Tang: 0000-0002-0293-964X

Notes

The authors declare no competing financial interest.

ACKNOWLEDGMENTS

This work has been partially supported by the National Basic Research Program of China (973 Program; 2013CB834701 and 2013CB834702), the University Grants Committee of Hong Kong (AoE/P-03/08), the National Science Foundation of China (21490570 and 21490574), the Research Grants Council of Hong Kong (16308116, 16308016, 16303815, N-HKUST604/14 and A-HKUST605/16), the Innovation and Technology Commission (ITC-CNERC14S01), and the Science and Technology Plan of Shenzhen (JCYJ20140425170011516 and JCYJ20160229205601482). B.Z.T. thanks the support of the Guangdong Innovative Research Team Program (201101C0105067115) and the Shenzhen Peacock.

DOI: 10.1021/acs.macromol.7b00973
Macromolecules 2017, 50, 5807−5815

REFERENCES

(1) White, J. L.; Bumm, S. H. Polymer Blend Compounding and Processing. In *Encyclopedia of Polymer Blends*; Isayev, A. I., Palsule, S., Eds.; Wiley-VCH: Weinheim, 2011; pp 1−26.

(2) Goettler, L. A.; Scobbo, Jr., J. J. Applications of Polymer Blends. In *Polymer Blends Handbook*, 2nd ed.; Utracki, L. A., Wilkie, C., Eds.; Springer: Netherlands, 2014; pp 1433−1458.

(3) Robeson, L. M. Fundamentals of Polymer Blends. In *Polymer Blends: A Comprehensive Review*; Robeson, L. M., Ed.; Hanser: Munich, 2007; pp 11−24.

(4) Jyotishkumar, P.; Thomas, S.; Grohens, Y. Polymer Blends: State of the Art, New Challenges, and Opportunities. In *Characterization of Polymer Blends: Miscibility, Morphology, and Interfaces*, 1st ed.; Thomas, S., Grohens, Y., Jyotishkumar, P., Eds.; Wiley-VCH: Weinheim, 2015; pp 1−5.

(5) Paul, D. R. Control of Phase Structure in Polymer Blends. In *Functional Polymers*; Bergbreiter, D. E., Martin, C. R., Eds.; Plenum Press: New York, 1989; pp 1−18.

(6) Paul, D. R. Polymer Blends: Phase Behavior and Property Relationships. In *Multicomponent Polymer Materials*; Paul, D. R., Sperling, L. H., Eds.; Advances in Chemistry; American Chemical Society: Washington, DC, 1985; pp 3−19.

(7) Moons, E. Conjugated Polymer Blends: Linking Film Morphology to Performance of Light Emitting Diodes and Photodiodes. *J. Phys.: Condens. Matter* **2002**, *14*, 12235−12260.

(8) Wenzl, F. P.; Pachler, P.; Suess, C.; Haase, A.; List, E. J. W.; Poelt, P.; Somitsch, D.; Knoll, P.; Scherf, U.; Leising, G. The Influence of the Phase Morphology on the Optoelectronic Properties of Light-Emitting Electrochemical Cells. *Adv. Funct. Mater.* **2004**, *14*, 441−450.

(9) Slota, J. E.; Elmalem, E.; Tu, G. L.; Watts, B.; Fang, J. F.; Oberhumer, P. M.; Friend, R. H.; Huck, W. T. S. Oligomeric Compatibilizers for Control of Phase Separation in Conjugated Polymer Blend Films. *Macromolecules* **2012**, *45*, 1468−1475.

(10) Liu, Y. H.; Zhao, J. B.; Li, Z. K.; Mu, C.; Ma, W.; Hu, H. W.; Jiang, K.; Lin, H. R.; Ade, H.; Yan, H. Aggregation and Morphology Control Enables Multiple Cases of High-Efficiency Polymer Solar Cells. *Nat. Commun.* **2014**, *5*, 5293.

(11) Sawyer, L. C.; Grubb, D. T.; Meyers, G. F. Applications of Microscopy to Polymers. In *Polymer Microscopy*, 3rd ed.; Sawyer, L. C., Grubb, D. T., Meyers, G. F., Eds.; Springer-Verlag: Berlin, 2008; pp 248−434.

(12) Xue, L. J.; Li, W. Z.; Hoffmann, G. G.; Goossens, J. G. P.; Loos, J.; de With, G. High-Resolution Chemical Identification of Polymer Blend Thin Films Using Tip-Enhanced Raman Mapping. *Macromolecules* **2011**, *44*, 2852−2858.

(13) Biria, S.; Hosein, I. D. Control of Morphology in Polymer Blends through Light Self-Trapping: An in Situ Study of Structure Evolution, Reaction Kinetics, and Phase Separation. *Macromolecules* **2017**, *50*, 3617−3626.

(14) Bernasik, A.; Rysz, J.; Budkowski, A.; Kowalski, K.; Camra, J.; Jedlinski, J. Three-Dimensional Information on the Phase Domain Structure of Thin Films of Polymer Blends Revealed by Secondary Ion Mass Spectrometry. *Macromol. Rapid Commun.* **2001**, *22*, 829−834.

(15) Momose, A.; Fujii, A.; Kadowaki, H.; Jinnai, H. Three-Dimensional Observation of Polymer Blend by X-Ray Phase Tomography. *Macromolecules* **2005**, *38*, 7197−7200.

(16) Adhikari, R. Electron Microscopic Analysis of Multicomponent Polymers and Blends. In *Characterization of Polymer Blends: Miscibility, Morphology, and Interfaces*, 1st ed.; Thomas, S., Grohens, Y., Jyotishkumar, P., Eds.; Wiley-VCH: Weinheim, 2015; pp 551−578.

(17) Roose, J.; Leung, A. C. S.; Wang, J.; Peng, Q.; Sung, H. H. Y.; Williams, I. D.; Tang, B. Z. A Colour-Tunable Chiral AIEgen: Reversible Coordination, Enantiomer Discrimination and Morphology Visualization. *Chem. Sci.* **2016**, *7*, 6106−6114.

(18) Chou, T. M.; Prayoonthong, P.; Aitouchen, A.; Libera, M. Nanoscale Artifacts in RuO_4-Stained Poly(styrene). *Polymer* **2002**, *43*, 2085−2088.

(19) Kim, S. H.; Kim, K. S.; Char, K.; Yoo, S. I.; Sohn, B. H. Short-Range Ordered Photonic Structures of Lamellae-Forming Diblock Copolymers for Excitation-Regulated Fluorescence Enhancement. *Nanoscale* **2016**, *8*, 10823−10831.

(20) Andrew, P.; Huck, W. T. S. Polymer Phase Separation on Lattice Patterned Surfaces. *Soft Matter* **2007**, *3*, 230−237.

(21) Guo, X.; Liu, L.; Zhuang, Z.; Chen, X.; Ni, M. Y.; Li, Y.; Cui, Y. S.; Zhan, P.; Yuan, C. S.; Ge, H. X.; Wang, Z. L.; Chen, Y. F. A New Strategy of Lithography Based on Phase Separation of Polymer Blends. *Sci. Rep.* **2015**, *5*, 15947.

(22) Serrano, B.; Baselga, J.; Bravo, J.; Mikes, F.; Sese, L.; Esteban, I.; Pierola, I. F. Chemical Imaging of Phase-Separated Polymer Blends by Fluorescence Microscopy. *J. Fluoresc.* **2000**, *10*, 135−139.

(23) Aoki, H. Fluorescence Microscopy Techniques for the Structural Analysis of Polymer Materials. In *Characterization of Polymer Blends: Miscibility, Morphology, and Interfaces*, 1st ed.; Thomas, S., Grohens, Y., Jyotishkumar, P., Eds.; Wiley-VCH: Weinheim, 2015; pp 609−624.

(24) Cabanelas, J. C.; Serrano, B.; Gonzalez, M. G.; Baselga, J. Confocal Microscopy Study of Phase Morphology Evolution in Epoxy/Polysiloxane Thermosets. *Polymer* **2005**, *46*, 6633−6639.

(25) Birks, J. B. *Photophysics of Aromatic Molecules*; Wiley: London, 1970.

(26) Levitsky, I.; Krivoshlykov, S. G.; Grate, J. W. Rational Design of a Nile Red/Polymer Composite Film for Fluorescence Sensing of Organophosphonate Vapors Using Hydrogen Bond Acidic Polymers. *Anal. Chem.* **2001**, *73*, 3441−3448.

(27) Doroshenko, M.; Gonzales, M.; Best, A.; Butt, H. J.; Koynov, K.; Floudas, G. Monitoring the Dynamics of Phase Separation in a Polymer Blend by Confocal Imaging and Fluorescence Correlation Spectroscopy. *Macromol. Rapid Commun.* **2012**, *33*, 1568−1573.

(28) Luo, J. D.; Xie, Z. L.; Lam, J. W. Y.; Cheng, L.; Chen, H. Y.; Qiu, C. F.; Kwok, H. S.; Zhan, X. W.; Liu, Y. Q.; Zhu, D. B.; Tang, B. Z. Aggregation-Induced Emission of 1-Methyl-1,2,3,4,5-Pentaphenylsilole. *Chem. Commun.* **2001**, 1740−1741.

(29) Mei, J.; Leung, N. L. C.; Kwok, R. T. K.; Lam, J. W. Y.; Tang, B. Z. Aggregation-Induced Emission: Together We Shine, United We Soar! *Chem. Rev.* **2015**, *115*, 11718−11940.

(30) Li, J. W.; Li, Y.; Chan, C. Y. K.; Kwok, R. T. K.; Li, H. K.; Zrazhevskiy, P.; Gao, X. H.; Sun, J. Z.; Qin, A. J.; Tang, B. Z. An Aggregation-Induced-Emission Platform for Direct Visualization of Interfacial Dynamic Self-Assembly. *Angew. Chem., Int. Ed.* **2014**, *53*, 13518−13522.

(31) Wang, Z. K.; Nie, J. Y.; Qin, W.; Hu, Q. L.; Tang, B. Z. Gelation Process Visualized by Aggregation-Induced Emission Fluorogens. *Nat. Commun.* **2016**, *7*, 12033.

(32) Robb, M. J.; Li, W.; Gergely, R. C. R.; Matthews, C. C.; White, S. R.; Sottos, N. R.; Moore, J. S. A Robust Damage-Reporting Strategy for Polymeric Materials Enabled by Aggregation-Induced Emission. *ACS Cent. Sci.* **2016**, *2*, 598−603.

(33) Guan, W. J.; Wang, S.; Lu, C.; Tang, B. Fluorescence Microscopy as an Alternative to Electron Microscopy for Microscale Dispersion Evaluation of Organic-Inorganic Composites. *Nat. Commun.* **2016**, *7*, 11811.

(34) Coran, A. Y. Thermoplastic Elastomeric Rubber-Plastic Blends. In *Handbook of Elastomers*, 2nd ed.; Bhowmick, A. K., Stephens, H., Eds.; Marcel Dekker. Inc.: New York, 2000; pp 265−320.

(35) Mei, J.; Hong, Y. N.; Lam, J. W. Y.; Qin, A. J.; Tang, Y. H.; Tang, B. Z. Aggregation-Induced Emission: The Whole Is More Brilliant Than the Parts. *Adv. Mater.* **2014**, *26*, 5429−5479.

(36) Iasilli, G.; Battisti, A.; Tantussi, F.; Fuso, F.; Allegrini, M.; Ruggeri, G.; Pucci, A. Aggregation-Induced Emission of Tetraphenylethylene in Styrene-Based Polymers. *Macromol. Chem. Phys.* **2014**, *215*, 499−506.

(37) Bao, S. P.; Wu, Q. H.; Qin, W.; Yu, Q. L.; Wang, J.; Liang, G. D.; Tang, B. Z. Sensitive and Reliable Detection of Glass Transition of Polymers by Fluorescent Probes Based on AIE Luminogens. *Polym. Chem.* **2015**, *6*, 3537−3542.

(38) Cascone, M. G.; Sim, B.; Sandra, D. Blends of Synthetic and Natural Polymers as Drug Delivery Systems for Growth Hormone. *Biomaterials* **1995**, *16*, 569−574.

DOI: 10.1021/acs.macromol.7b00973
Macromolecules 2017, 50, 5807−5815

(39) Mi, F. L.; Lin, Y. M.; Wu, Y. B.; Shyu, S. S.; Tsai, Y. H. Chitin/PLGA Blend Microspheres as a Biodegradable Drug-Delivery System: Phase-Separation, Degradation and Release Behavior. *Biomaterials* **2002**, *23*, 3257−3267.
(40) Munj, H. R.; Nelson, M. T.; Karandikar, P. S.; Lannutti, J. J.; Tomasko, D. L. Biocompatible Electrospun Polymer Blends for Biomedical Applications. *J. Biomed. Mater. Res., Part B* **2014**, *102*, 1517−1527.
(41) Serra, T.; Ortiz-Hernandez, M.; Engel, E.; Planell, J. A.; Navarro, M. Relevance of PEG in PLA-Based Blends for Tissue Engineering 3D-Printed Scaffolds. *Mater. Sci. Eng., C* **2014**, *38*, 55−62.
(42) Tipduangta, P.; Belton, P.; Fabian, L.; Wang, L. Y.; Tang, H. R.; Eddleston, M.; Qi, S. Electrospun Polymer Blend Nanofibers for Tunable Drug Delivery: The Role of Transformative Phase Separation on Controlling the Release Rate. *Mol. Pharmaceutics* **2016**, *13*, 25−39.
(43) Hurrell, S.; Cameron, R. E. The Effect of Initial Polymer Morphology on the Degradation and Drug Release from Polyglycolide. *Biomaterials* **2002**, *23*, 2401−2409.
(44) Yang, Z.; Nollenberger, K.; Albers, J.; Craig, D.; Qi, S. Microstructure of an Immiscible Polymer Blend and Its Stabilization Effect on Amorphous Solid Dispersions. *Mol. Pharmaceutics* **2013**, *10*, 2767−2680.
(45) Hu, R. R.; Lager, E.; Aguilar-Aguilar, A.; Liu, J. Z.; Lam, J. W. Y.; Sung, H. H. Y.; Williams, I. D.; Zhong, Y. C.; Wong, K. S.; Pena-Cabrera, E.; Tang, B. Z. Twisted Intramolecular Charge Transfer and Aggregation-Induced Emission of BODIPY Derivatives. *J. Phys. Chem. C* **2009**, *113*, 15845−15853.
(46) Sasaki, S.; Drummen, G. P. C.; Konishi, G. Recent Advances in Twisted Intramolecular Charge Transfer (TICT) Fluorescence and Related Phenomena in Materials Chemistry. *J. Mater. Chem. C* **2016**, *4*, 2731−2743.
(47) Zhang, Y. L.; Jiang, M. J.; Han, G. C.; Zhao, K.; Tang, B. Z.; Wong, K. S. Solvent Effect and Two-Photon Optical Properties of Triphenylamine-Based Donor-Acceptor Fluorophores. *J. Phys. Chem. C* **2015**, *119*, 27630−27638.

DOI: 10.1021/acs.macromol.7b00973
Macromolecules 2017, 50, 5807−5815